Lifetime and size of shallow magma bodies controlled by crustal-scale magmatism

Ozge Karakas[1*], Wim Degruyter[2], Olivier Bachmann[1], and Josef Dufek[3]

[1]Department of Earth Sciences, Institute of Geochemistry and Petrology, ETH Zurich, Clausiusstrasse 25, CH-8092, Zurich, Switzerland

[2]School of Earth and Ocean Sciences, Cardiff University, Main Building, Park Place, Cardiff, CF10 3AT, Wales, UK

[3]School of Earth and Atmospheric Sciences, Georgia Institute of Technology, 311 Ferst Drive, Atlanta, GA 30332, USA

Magmatic processes on Earth govern the mass, energy, and chemical transfer between the mantle, crust, and atmosphere. To understand magma storage conditions in the crust that ultimately control volcanic activity and growth of continents, an evaluation of the mass and heat budget of the entire crustal column during magmatic episodes is essential. Here we use a numerical model to constrain the physical conditions under which both lower and upper crustal magma bodies form. We find that over long durations of intrusions (greater than 10^5-10^6 yr), extensive lower crustal mush zones develop, which modify the thermal budget of the upper crust and reduce the flux of magma required to sustain upper crustal magma reservoirs. Our results reconcile physical models of magma reservoir construction and field-based estimates of intrusion rates in numerous volcanic and plutonic localities. Young igneous provinces (less than a few 100 kyr old) are unlikely to support large upper crustal reservoirs, whereas longer-lived systems (active for

longer than 1 Myr) can accumulate magma and build reservoirs capable of producing supereruptions, even with intrusion rates smaller than 10^{-3}-10^{-2} km^3/yr. Hence, total duration of magmatism should be combined with the magma intrusion rates to assess the capability of volcanic systems to form the largest explosive eruptions on Earth.

Magma reservoirs within the continental upper crust are key locations to generate the most viscous and potentially explosive magmas on Earth[1-4]. How they form and how long they remain eruptible, continues to be a matter of lively debate. Published lifetimes of eruptible portions within such reservoirs range from centuries to hundreds of thousands of years[5-15], leading to controversial implications for volcanic hazard and for the link between volcanic and plutonic lithologies[16,17]. Studies arguing for long-lived magma reservoirs often depict large, highly crystalline regions in the upper crust ("mush zones"; ref.18) from which melt-rich, eruptible pockets can be extracted[3,18-20]. In contrast, others suggest that mobile magma bodies are ephemeral features that assemble from deep sources and erupt on short timescales[11,21,22] or solidify to form plutonic rocks[23,24].

At the crux of this debate is the magma intrusion rate required to maintain magma bodies above the solidus in the crust[23,25-29]. In the cold upper crust (~5-15 km deep), existing numerical thermal models require high intrusion rates ($\geq 10^{-2}$ km^3/yr, ref. 23; $\geq 5\times10^{-3}$ km^3/yr, ref. 29), to produce eruptible pockets of magma, leading to short timescales of magma accumulation, even for supereruptions ($<10^4$-10^5 yr). This is incongruous with geological estimates of such rates, which are typically lower[25,27,28]. High intrusion rates also impose decoupling of volcanic and plutonic realms, leading to either large erupted volumes[23,30] or relatively small plutons[30]. Moreover, mechanical

models show that the highest rates implied by thermal models (~$\geq 10^{-2}$ km^3/yr) are unlikely to sustain large magma bodies in the upper crust because associated overpressure would trigger eruptions before large amounts of magma can accumulate[31] (the "room" problem). In order to generate large, crustal-scale magmatic columns without losing too much mass to volcanic output, magma emplacement must be prolonged at relatively low intrusion rates[31].

Modelling of magma intrusions at crustal-scale

A fundamental aspect of upper crustal magma storage that has not been considered in previous thermal models[23,26,29] is the presence of lower crustal magma reservoirs. Petrological and geophysical evidence supports large accumulations of magma in the lower crust of many volcanic regions[32-36], which can be active for millions of years[27,37,38]. However, the effect of these lower crustal magma reservoirs on the upper crustal thermal structure has not been systematically quantified (see, however, Extended Data Fig. 1 and ref. 39 for mid-crustal sill). We bridge this gap and use an existing model[40] of stochastic and incremental injections of magma (as dikes and sills) to consider the thermal influence of lower crustal reservoirs on the upper continental crust over long timescales (>10^5 yr) and footprints (areas through which dykes/sills are injected) of >10^2-10^3 km^2. We focus on a two-dimensional generic crustal column (~30 km thick) and its underlying mantle (Fig. 1, and see Methods). In order to quantify the thermal evolution of the entire magmatic province over geological timescales (10^5-10^6 yr), the simulations are run in two stages:

- Stage I. Emplacement of basaltic magma (~≥10^{-2} km^3/yr) in the lower crust over relatively long timescales (>10^6 yr), as inferred in many continental settings[25,38,41,42].
- Stage II. Emplacement of intermediate magma in the upper crust in both small (~10^2 km^2 footprint) and large systems (~10^3 km^2 footprint). Simulation duration is set between 10^5 and 10^6 yr, depending on the magma flux. In this stage, we use the upper crustal thermal structure determined from stage I as the new initial condition.

In stage I, basaltic dikes and sills are incrementally emplaced in the lower crust (see Methods for geometry and compositions used). This leads to a significant temperature increase within the whole crust after ~3-4 Myr of intrusions (Fig. 2), and a lower crustal mush zone forms that is comparable in size to field[36] and seismic[32,34] estimates in magmatic provinces (e.g., ~45 km width at Yellowstone Caldera, ref. 32). At this point, the upper crustal thermal gradient reaches near steady state (Fig. 2b inset; Fig 2a, d) conductive gradient, implying that the average temperature in the upper crust does not change significantly after this timescale (<0.5%; with a nearly constant heat flux between the lower and upper crust). In this study, we refer to this timescale as the 'thermal maturation timescale'.

In stage II, we quantify the generation and storage of upper crustal magma bodies using three different initial upper crustal thermal profiles: 1) without a lower crustal heating source, referred to as the 'undisturbed geotherm' (Fig 2c), 2) after the lower crustal mush has grown for 1 Myr, referred to as 'thermally juvenile' upper crust, and 3) after the lower crustal mush has grown for 4 Myr, referred to as 'thermally mature' upper

crust (Fig 2b, d). We vary the upper crustal magma flux between 10^{-6} and 10^{-5} $km^3/km^2/yr$ (equivalent to rates of ~10^{-4} to ~10^{-2} km^3/yr) and total upper crustal intrusion timescales for >10^5-10^6 yr. These fluxes and durations are consistent with the amount of melt available in the lower crustal mush zones (see Methods). We refer to magma intrusion rates on the order of ~10^{-2} km^3/yr as 'high', ~10^{-3} km^3/yr as 'intermediate', and ~10^{-4} km^3/yr as 'low' rates.

Longevity and size of upper crustal magma systems

The presence of a lower crustal mush system strongly impacts the generation and storage conditions of upper crustal magma reservoirs. When using an undisturbed geotherm (i.e., absence of a lower crustal mush), we find that the critical upper crustal magma flux (minimum flux necessary to keep the system above solidus) is >10^{-4} $km^3/km^2/yr$ (or a rate >10^{-2} km^3/yr for a footprint of ~10^2 km^2) in line with estimates of previous thermal models[23,29]. In stark contrast, when a lower crustal mush system has fully developed (thermally mature system), upper crustal magma bodies can survive in a mush state for long periods (>10^5 to 10^6 yr, in line with geochronological information[12,15,43,44]; Fig. 3). In these systems, the critical upper crustal magma flux significantly drops and ranges between 10^{-6} and 10^{-5} $km^3/km^2/yr$ (or a rate of ~10^{-4} to 10^{-3} km^3/yr for a footprint of ~10^2 km^2; Fig. 3, Extended Data Fig. 2), consistent with observations from several magmatic provinces[25,27].

Thermal maturation of the upper crust

The remarkable similarity between erupted fluxes calculated for "flare-up" regions[27] (characterized by a series of caldera-forming eruptions clustered in time that evacuate >10^4 km^3 of silicic magma) and average rates of typical arc volcanoes[25,45]

suggests that, rather than rates alone, the duration of magma intrusion in the upper crust plays a dominant role in the size of magma reservoirs, and ultimately in the volume of erupted material (Figs. 3b, 4). When magma bodies are maintained in a partially molten state (i.e., magma flux is larger than the critical flux), successive magma emplacements in the upper crust can develop voluminous subvolcanic reservoirs, given enough time[46] (Fig. 3b). In both thermally juvenile (1 Myr of lower crustal magmatism) and thermally mature (4 Myr of lower crustal magma evolution) conditions, the total duration of lower and upper crustal magmatism is between 1.5 to 7 Myr, on par with geochronological estimates on various volcanic provinces[41,42]. Within the range of geologically observed upper crustal magma fluxes[27,28] (10^{-5} to 10^{-6} $km^3/km^2/yr$, rates ~10^{-4} to ~10^{-2} km^3/yr), a broad range of volumes of upper crustal reservoirs can be formed as a function of the maturation timescale (i.e., thermally juvenile or mature upper crust) and duration of upper crustal magmatism (Fig. 4). Our calculations show that:

- Regions that are relatively young (~10^4-10^5 yr, smaller footprints ~10^2 km^2, Fig. 4) generate only small eruptions of intermediate to silicic magmas (if at all), leaving plutonic material with, on average, limited to no cumulate signature (not much melt extraction that feeds rhyolitic eruptions), at least in the upper crust.
- Regions that are long-lived (>10^5-10^6 yr, larger footprint ~10^3 km^2, Fig. 4) can produce large volumes of eruptible magma (>10^3 km^3), feeding supereruptions, and leaving behind significant amounts of intermediate to silicic cumulates[19] when rhyolites are produced[4].

- Between these extremes, the remaining range of volcanic and plutonic lithologies can be formed (Fig. 4).

Our unified framework for crustal-scale magmatic systems helps provide a sharper understanding of the differentiation and growth of the continental crust, the volcanic-plutonic connection, and the volume and lifetime of magma plumbing systems that pose significant volcanic hazards. The rarity of supereruptions need not be due to exceptionally high transient magma fluxes[48], but to intermediate fluxes that last for long periods of time (million-year timescale, see Methods). Such a scenario is more compatible with a multitude of observations and physical constraints, not the least being the "room problem". The continental crust is capable of accommodating large, albeit mostly crystalline, magma bodies, at multiple levels (polybaric differentiation[4,27,33,49-51]), as long as it has the time to do so. In such conditions, extensive tectonic extension is not even required. Large mush zones first grow in the lower crust, generating buoyant derivative melts of intermediate compositions (mostly andesite/dacite) that can ascend towards the surface. As the crustal column thermally matures, the upper crust becomes warm enough to make the room for its own mush zones, where the most evolved, commonly explosive magmas on Earth (rhyolites) can be produced. In magmatic provinces that build over millions of years with significant (but not extreme) fluxes of mafic to intermediate magmas, rhyolitic melt can accumulate in large volumes in the upper crustal mush zones, and produce the largest caldera-forming eruptions in the geological record.

References

1 Sparks, R., Huppert, H., Turner, J., Sakuyama, M. & O'Hara, M. The fluid dynamics of evolving magma chambers [and discussion]. *Philosophical Transactions of the Royal Society of London A: Mathematical, Physical and Engineering Sciences* **310**, 511-534 (1984).

2 Marsh, B. D. Magma chambers. *Annual Review of Earth and Planetary Sciences* **17**, 439-472 (1989).

3 Bachmann, O. & Huber, C. Silicic magma reservoirs in the Earth's crust. *American Mineralogist* **101**, 2377-2404 (2016).

4 Bachmann, O. & Bergantz, G. W. Rhyolites and their Source Mushes across Tectonic Settings. *Journal of Petrology* **49**, 2277-2285, doi:10.1093/petrology/egn068 (2008).

5 Claiborne, L. L., Miller, C. F., Flanagan, D. M., Clynne, M. A. & Wooden, J. L. Zircon reveals protracted magma storage and recycling beneath Mount St. Helens. *Geology* **38**, 1011-1014 (2010).

6 Costa, F. Residence times of silicic magmas associated with calderas. *Developments in volcanology* **10**, 1-55 (2008).

7 Eddy, M. P., Bowring, S. A., Miller, R. B. & Tepper, J. H. Rapid assembly and crystallization of a fossil large-volume silicic magma chamber. *Geology* **44**, 331-334 (2016).

8 Schoene, B. *et al.* Rates of magma differentiation and emplacement in a ballooning pluton recorded by U–Pb TIMS-TEA, Adamello batholith, Italy. *Earth and Planetary Science Letters* **355**, 162-173 (2012).

9 Memeti, V., Paterson, S., Matzel, J., Mundil, R. & Okaya, D. Magmatic lobes as "snapshots" of magma chamber growth and evolution in large, composite batholiths: An example from the Tuolumne intrusion, Sierra Nevada, California. *Geological Society of America Bulletin* **122**, 1912-1931 (2010).

10 Barboni, M. & Schoene, B. Short eruption window revealed by absolute crystal growth rates in a granitic magma. *Nature Geoscience* (2014).

11 Pamukcu, A. S., Gualda, G. A., Bégué, F. & Gravley, D. M. Melt inclusion shapes: Timekeepers of short-lived giant magma bodies. *Geology* **43**, 947-950 (2015).

12 Reid, M. R., Coath, C. D., Harrison, T. M. & McKeegan, K. D. Prolonged residence times for the youngest rhyolites associated with Long Valley Caldera: 230 Th—238 U ion microprobe dating of young zircons. *Earth and Planetary Science Letters* **150**, 27-39 (1997).

13 Druitt, T., Costa, F., Deloule, E., Dungan, M. & Scaillet, B. Decadal to monthly timescales of magma transfer and reservoir growth at a caldera volcano. *Nature* **482**, 77-80 (2012).

14 Parks, M. M. *et al.* Evolution of Santorini Volcano dominated by episodic and rapid fluxes of melt from depth. *Nature Geoscience* **5**, 749-754 (2012).

15 Kaiser, J. F., de Silva, S., Schmitt, A. K., Economos, R. & Sunagua, M. Million-year melt–presence in monotonous intermediate magma for a volcanic–plutonic assemblage in the Central Andes: Contrasting histories of crystal-rich and crystal-poor super-sized silicic magmas. *Earth and Planetary Science Letters* **457**, 73-86 (2017).

16 Keller, C. B., Schoene, B., Barboni, M., Samperton, K. M. & Husson, J. M. Volcanic-plutonic parity and the differentiation of the continental crust. *Nature* **523**, 301-307, doi:10.1038/nature14584 (2015).

17 Deering, C. D. *et al.* Zircon record of the plutonic-volcanic connection and protracted rhyolite melt evolution. *Geology*, G37539. 37531 (2016).

18 Hildreth, W. Volcanological perspectives on Long Valley, Mammoth Mountain, and Mono Craters: several contiguous but discrete systems. *Journal of Volcanology and Geothermal Research* **136**, 169-198, doi:10.1016/j.volgrores.2004.05.019 (2004).

19 Gelman, S. E., Deering, C. D., Bachmann, O., Huber, C. & Gutiérrez, F. J. Identifying the crystal graveyards remaining after large silicic eruptions. *Earth and Planetary Science Letters* **403**, 299-306 (2014).

20 Lee, C. T. A. & Bachmann, O. How important is the role of crystal fractionation in making intermediate magmas? Insights from Zr and P systematics. *Earth Planet. Sci. Lett.* **393**, 266-274 (2014).

21 Menand, T., Annen, C. & de Saint Blanquat, M. Rates of magma transfer in the crust: Insights into magma reservoir recharge and pluton growth. *Geology* **43**, 199-202 (2015).

22 Wotzlaw, J.-F., Bindeman, I. N., Stern, R. A., D'Abzac, F.-X. & Schaltegger, U. Rapid heterogeneous assembly of multiple magma reservoirs prior to Yellowstone supereruptions. *Scientific reports* **5** (2015).

23 Annen, C. From plutons to magma chambers: thermal constraints on the accumulation of eruptible silicic magma in the upper crust. *Earth Planet. Sci. Lett.* **284**, 409-416 (2009).

24 Glazner, A. F., Bartley, J. M., Coleman, D. S., Gray, W. & Taylor, R. Z. Are plutons assembled over millions of years by amalgamation from small magma chambers? *GSA today* **14**, 4-12 (2004).

25 White, S. M., Crisp, J. A. & Spera, F. J. Long-term volumetric eruption rates and magma budgets. *Geochemistry, Geophysics, Geosystems* **7** (2006).

26 Paterson, S. R., Okaya, D., Memeti, V., Economos, R. & Miller, R. B. Magma addition and flux calculations of incrementally constructed magma chambers in continental margin arcs: Combined field, geochronologic, and thermal modeling studies. *Geosphere* **7**, 1439-1468 (2011).

27 Lipman, P. W. & Bachmann, O. Ignimbrites to batholiths: Integrating perspectives from geological, geophysical, and geochronological data. *Geosphere* **11**, 705-743 (2015).

28 Dimalanta, C., Taira, A., Yumul, G. P., Tokuyama, H. & Mochizuki, K. New rates of western Pacific island arc magmatism from seismic and gravity data. *Earth and Planetary Science Letters* **202**, 105-115, doi:10.1016/s0012-821x(02)00761-6 (2002).

29 Gelman, S. E., Gutiérrez, F. J. & Bachmann, O. On the longevity of large upper crustal silicic magma reservoirs. *Geology* **41**, 759-762 (2013).

30 Caricchi, L., Simpson, G. & Schaltegger, U. Zircons reveal magma fluxes in the Earth/'s crust. *Nature* **511**, 457-461 (2014).

31 Jellinek, A. M. & DePaolo, D. J. A model for the origin of large silicic magma chambers: precursors of caldera-forming eruptions. *Bulletin of Volcanology* **65**, 363-381 (2003).

32 Huang, H.-H. *et al.* The Yellowstone magmatic system from the mantle plume to the upper crust. *Science*, aaa5648 (2015).

33 Hildreth, W. & Moorbath, S. Crustal contributions to arc magmatism in the Andes of central Chile *Contributions to Mineralogy and Petrology* **98**, 455-489, doi:10.1007/bf00372365 (1988).

34 Kiser, E. *et al.* Magma reservoirs from the upper crust to the Moho inferred from high-resolution Vp and Vs models beneath Mount St. Helens, Washington State, USA. *Geology*, G37591. 37591 (2016).

35 Walker, B. A., Bergantz, G. W., Otamendi, J. E., Ducea, M. N. & Cristofolini, E. A. A MASH zone revealed: the mafic complex of the Sierra Valle Fértil. *Journal of Petrology* **56**, 1863-1896 (2015).

36 Jagoutz, O. & Schmidt, M. W. The composition of the foundered complement to the continental crust and a re-evaluation of fluxes in arcs. *Earth and Planetary Science Letters* **371**, 177-190, doi:10.1016/j.epsl.2013.03.051 (2013).

37 Coint, N., Barnes, C., Yoshinobu, A., Chamberlain, K. & Barnes, M. Batch-wise assembly and zoning of a tilted calc-alkaline batholith: Field relations, timing, and compositional variation. *Geosphere* **9**, 1729-1746 (2013).

38 Grunder, A. L., Klemetti, E. W., Feeley, T. C. & McKee, C. M. Eleven million years of arc volcanism at the Aucanquilcha Volcanic Cluster, northern Chilean

Andes: implications for the life span and emplacement of plutons. *Transactions of the Royal Society of Edinburgh: Earth Sciences* **97**, 415-436 (2006).

39 de Silva, S. L. & Gregg, P. M. Thermomechanical feedbacks in magmatic systems: Implications for growth, longevity, and evolution of large caldera-forming magma reservoirs and their supereruptions. *Journal of Volcanology and Geothermal Research* **282**, 77-91 (2014).

40 Dufek, J. & Bergantz, G. W. Lower crustal magma genesis and preservation: A stochastic framework for the evaluation of basalt-crust interaction. *Journal of Petrology* **46**, 2167-2195, doi:10.1093/petrology/egi049 (2005).

41 Ducea, M. N., Bergantz, G. W., Crowley, J. L. & Otamendi, J. Ultrafast magmatic buildup and diversification to produce continental crust during subduction. *Geology*, G38726. 38721 (2017).

42 Quick, J. *et al.* Magmatic plumbing of a large Permian caldera exposed to a depth of 25 km. *Geology* **37**, 603-606 (2009).

43 Frazer, R. E., Coleman, D. S. & Mills, R. D. Zircon U-Pb geochronology of the Mount Givens Granodiorite: Implications for the genesis of large volumes of eruptible magma. *Journal of Geophysical Research: Solid Earth* **119**, 2907-2924 (2014).

44 Barboni, M. *et al.* Warm storage for arc magmas. *Proceedings of the National Academy of Sciences* **113**, 13959-13964 (2016).

45 de Saint Blanquat, M. *et al.* Multiscale magmatic cyclicity, duration of pluton construction, and the paradoxical relationship between tectonism and plutonism in continental arcs. *Tectonophysics* **500**, 20-33 (2011).

46 Degruyter, W., Huber, C., Bachmann, O., Cooper, K. M. & Kent, A. J. Magma reservoir response to transient recharge events: The case of Santorini volcano (Greece). *Geology* **44**, 23-26 (2016).

47 Glazner, A. F., Bartley, J. M., Coleman, D. S., Gray, W. & Taylor, R. Z. Are plutons assembled over millions of years by amalgamation from small magma chambers? *GSA Today* **14**, 4-11 (2004).

48 Annen, C., Blundy, J. D., Leuthold, J. & Sparks, R. S. J. Construction and evolution of igneous bodies: Towards an integrated perspective of crustal magmatism. *Lithos* **230**, 206-221 (2015).

49 Lipman, P. W., Doe, B. R., Hedge, C. E. & Steven, T. A. Petrologic evolution of San-Juan volcanic field, southwestern Colorado - Pb and Sr isotope evidence *Geological Society of America Bulletin* **89**, 59-82, doi:10.1130/0016-7606(1978)89<59:peotsj>2.0.co;2 (1978).

50 Melekhova, E., Blundy, J., Robertson, R. & Humphreys, M. C. S. Experimental Evidence for Polybaric Differentiation of Primitive Arc Basalt beneath St. Vincent, Lesser Antilles. *Journal of Petrology* **56**, 161-192, doi:10.1093/petrology/egu074 (2015).

51 Annen, C., Blundy, J. D. & Sparks, R. S. J. The genesis of intermediate and silicic magmas in deep crustal hot zones. *Journal of Petrology* **47**, 505-539 (2006).

Acknowledgements We thank Christian Huber and George Bergantz for their help over the years. O.K. and O.B. acknowledge the support from Swiss SNF project 200020_165501. O.K. and J.D. acknowledge the support from NSF grant EAR 1321843.

Author contributions The conceptual model was developed by O.K., W.D., and O.B. The original numerical model was developed by J.D. and adapted and executed by O.K. for this study. All authors contributed to the writing of the manuscript, with O.K. taking the lead.

Additional information A detailed description of the two-dimensional implicit finite volume model is given in the Methods. Correspondence and requests for materials should be addressed to O.K. (ozge.karakas@erdw.ethz.ch).

Competing financial interests The authors declare no competing financial interests.

Figure captions:

Figure 1 | Geometry of the numerical model. The computational domain consists of the crust and upper mantle. The upper crust (uppermost 15 km) is considered tonalitic, while the lower crust (between 15-30 km) is amphibolitic, and the upper mantle (between 30-60 km) peridotitic. Drawing is not to scale. All the parameters and assumptions used in the model are outlined in the methods section.

Figure 2 | Thermal evolution of the crust in response to lower crustal dike and sill intrusions. a, Mean temperature of the crust and the upper mantle over time. **b,** Thermal maturation timescales in the upper crust as a function of lower crustal magma flux. The upper crust is defined as 'thermally mature' when the rate of change of average upper crustal temperature (ºC) becomes <0.5% (inset figure). **c,** Initial two-dimensional

temperature distribution in the crust. **d,** Two-dimensional temperature distribution after 4 Myr of lower crustal dike and sill injections. Simulated areas of previous upper crustal thermal calculations of refs. 23 and 29 are shown with dashed lines in **c** and **d**.

Figure 3 | Normalized volume of magma in the upper crust as a function magma flux and time. a, Upper crustal magma flux and normalized magma volume (divided by the intruded area) that can form 'eruptible' magma bodies (melt fraction > 0.6) in the upper crust. Note the difference in timescales in different scenarios. Results of refs. 23 and 29 for similar modeling conditions are included for comparison. The results of the undisturbed geotherm of this study reproduce the same range as ref. 29 and are lower than ref. 23 due to the use of a different melting curve. **b,** Upper crustal magma flux and normalized magma volume that can form 'mush' regions (melt fraction > 0.4) in the upper crust.

Figure 4 | Summary of the numerical results, showing duration and volume of upper crustal mush bodies (melt fraction >0.4) at different stages of maturation. Two different trends in the graph represent magmatic systems with different footprints (~10^2 km^2 and ~10^3 km^2). Natural examples: a, Large and long-lived systems such as Yellowstone and San Juan Volcanic Field, see refs. 27,43,45; b, Small and young systems such as Santorini, see refs 43, 45; c, Long-lived small to intermediate-sized batholiths, such as Adamello, see refs. 43, 45, 30. Results of previous numerical studies, in which lower crustal magma bodies are not considered, are shown with shaded areas. The area defined as supereruptions of ref. 23 takes the eruptible volume (melt fraction >0.6) from the time and volume range in a caldera system with 20 km diameter. The "large eruptions"

field from ref. 30 is taken directly from their Figure 4d, while their "plutonic" field was recalculated with their given fluxes and durations, in our simulations, to match our volume of "mush" (melt fraction >0.4).

Extended Data Figure 1 | Average temperature of the crust and uppermost mantle under incremental dike and sill intrusions until the thermal maturation of the upper crust is reached (4 Myr). Comparison of the temperature profile of current study conditions proposed for the thermal priming of the upper crust during the ignimbrite flare-up episodes of the Altiplano-Puna Volcanic Complex[39]. In this latter case, heat is supplied to the upper crust by advection at the base of the upper crust. This mechanism implies the instantaneous emplacement of a magma body in the mid-crust that would remain there at near-liquidus temperature for millions of years. Such conditions are geologically unrealistic as intrusions will cool to background temperatures within this timescale. In the present study, thermal maturation of the upper crust is not achieved by advection, but by conduction of heat coming from the incremental formation of the lower crustal magma body.

Extended Data Figure 2 | Volume of magma in upper crust as a function of upper crustal magma flux when the intruded volumes are ~3300 km^3 in all simulations. The magma volume is calculated by multiplying the two-dimensional results with the intruded width. Results of previous thermal models are given for comparison. The magma fluxes for refs. 23 and 29 studies are calculated by dividing their results by the intruded area, πr^2, where r is 10 km. Results of ref. 29 represent their calculations for

temperature-dependent thermal conductivity with sills of 10 km radius. Results of ref. 23 symbols show the calculations for sill intrusions of 10 km radius.

METHODS

We have adapted a two-dimensional thermal model[40,52] using a fully implicit finite volume scheme[53] to assess the thermal evolution of the crust that is subjected to incremental dike and sill intrusions. To investigate the entire crustal section, we simulate a domain that is 80 kilometers wide and 60 kilometers deep, with 40 meters resolution in both directions (Fig. 1). Initially, we identify a geotherm with radiogenic heating contribution that exponentially decays down to a depth of 12 km. The surface temperature is set at 0°C and mantle heat flux is fixed at 40 mW/m^2, corresponding to ~75 mW/m^2 initial surface heat flow, consistent with the average heat flow of crust of the modern Earth in different settings[54-56]. Initial steady-state geotherm of the crust is given by:

$$k\frac{\partial}{\partial x_1}\left(\frac{\partial T}{\partial x_1}\right)+\rho_{crust}H_0e^{(-x_1/L)}=0, \qquad (1)$$

where, T is temperature, k is heat conduction, ρ is density, H_0 is the radiogenic heat production (8×10^{-10} W/kg, constrained by refs. 57,58), and L is the characteristic depth for radiogenic element concentration decay (12 km, comparable to refs. 59,60). We assume that the uppermost 30 kilometers of the computational domain represents the initial crustal thickness and thickens up to 32 to 36 km in time depending on the magma flux. This crustal thickness is within the range of crustal thickness estimates from several volcanic regions[61]. Basaltic dikes and sills are emplaced in the lower crust for >10^6 yr in the lower crust. This configuration allows us to determine the thermal structure of the crust after long-term magma intrusions. From these temperature profiles, we define the thermal maturation time for the upper crust at different lower crustal magma fluxes. We find that for an intrusion rate of ~10^{-2} km^3/yr, the thermal maturation

time of the upper crust is ~4 Myr (comparable to diffusion timescales, $t=d^2/K$, where d is lengthscale and K is the thermal diffusivity constant). At that time, the total volume of melt in the lower crust is ~18,000 km^3. Extracting this volume of melt from the lower crust and intruding into the upper crust suggests a range of upper crustal intrusion rates ($<10^{-2}$ km^3/yr) over $>10^6$ years. We note that using the profile of other lower crustal fluxes will change the thermal maturation time, but the general trends presented in this study will be preserved. We then use the thermal structure defined at 4 Myr (with basalt intrusion rate of ~10^{-2} km^3/yr) as an initial condition for the upper crust, and intrude dikes and sills of intermediate composition in the upper crust between 5 and 15 km for $>10^5$-10^6 yr. We assume constant temperature boundary conditions for the computational domain in both stages. We also assume that dikes and sills are emplaced in the crust at their liquidus temperatures.

Incremental emplacement of dikes and sills is assumed to be a stochastic process as described in refs. 40,53. We use the L'Ecuyer random number generator algorithm[62] for stochastic behavior of the intrusions in time, volume, and space. The dikes are 160 m thick with varying lengths starting from the crust-mantle boundary and intrude up to 17 km. Sills are emplaced at the tip of dikes, and are 120 m thick with varying lengths ranging from 120 m to 3000 m. In the upper crust, dikes are 160 m width with lengths changing between depths of 15 and 5 km and sills are 120 m thick and with lengths ranging between 160 m and 1000 m. The stochastic nature of the model allows for different intrusion (dike/sill) lengths, timing, and location. The only parameter that is kept constant is the width of intrusions, which are comparable to dike thicknesses observed in nature[63]. As the thermal evolution of the crust is controlled by the heat input (average magma flux) rather than the individual dimensions, our choice of intrusion widths have negligible effects on the overall characteristics of the results as

shown in our previous studies[40]. The lower crustal dikes are randomly emplaced in the crust across the crust-mantle boundary, and the upper crustal dikes are randomly emplaced above 15 km depth. Following other thermal models, dike and sill emplacement is considered to be instantaneous relative to the cooling timescale. At each emplacement, mass is conserved by laterally moving the crust on both sides of the dike by a length that is equal to the half-width of the dike. Emplacement of sills is accommodated by subsiding the crustal material downward by the sill thickness.

Energy transported by emplaced dikes and sills diffuses in the surrounding crust that is colder. We simulate this by solving the conservation of enthalpy H:

$$\frac{\partial H}{\partial t} + \frac{\partial}{\partial x_j}(v_j H) = k\frac{\partial}{\partial x_i}\left(\frac{\partial T}{\partial x_i}\right) \tag{3.1}$$

where the first term is the time variation of the enthalpy, the second term is the advection term, and the last term denotes the heat loss by conduction. The enthalpy is partitioned into sensible heat and latent heat as follows

$$H = \rho_{mix}\int_{Tref}^{T} c_{mix}\,dT + \rho_{mix} f L \tag{3.2}$$

where the first term on the right hand side is the sensible heat and the second term describes the latent heat contribution to enthalpy change. We choose a latent heat value (L) of 4 x 10^5 J for the crystallizing magma. f is the melt fraction and its evolution over time is determined by the temperature and thus we can write

$$\frac{\partial f}{\partial t} = \frac{\partial f}{\partial T}\frac{\partial T}{\partial t}. \tag{3.3}$$

The mixture properties of the density (ρ), heat capacity (c), and thermal conductivity (k) parameters are assigned to lower crustal material, upper crustal material, basaltic magma, and intermediate magma and are calculated as follows

$$\rho_{mix} = \gamma f_c \rho_c^l + \gamma(1-f_c)\rho_c^s + (1-\gamma) f_i \rho_i^l + (1-\gamma)(1-f_i)\rho_i^s, \quad (3.4)$$

$$c_{mix} = \gamma f_c c_c^l + \gamma(1-f_c)c_c^s + (1-\gamma) f_i c_i^l + (1-\gamma)(1-f_i)c_i^s, \quad (3.5)$$

$$k_{mix} = \gamma f_c k_c^l + \gamma(1-f_c)k_c^s + (1-\gamma) f_i k_i^l + (1-\gamma)(1-f_i)k_i^s, \quad (3.6)$$

where γ is a parameter showing the volume fraction of crustal material or basalt at particular location at particular time ($\gamma=1$ denotes crustal material, $\gamma=0$ denotes intruded magma). Superscripts *l* and *s* refer to liquid and solid, and subscripts *c* and *i* refer to crust and intrusions, respectively. Appropriate values for these parameters are gathered from refs. 23, 29, 40, and 52.

Solving the energy equation requires accurate partitioning of total enthalpy to latent and sensible heat. The evolution of latent heat during melting and crystallization follows the liquid line of descent determined by petrologic experiments with different compositions and pressures. We assumed an average crustal dichotomy in composition between a lower mafic crust and upper silicic crust by taking (i) amphibolitic composition for the lower crust (15 to 30 km depth) and melt fraction-temperature relationships from experiments by ref. 64 and (ii) tonalitic composition for mid-upper crust (0 to 15 km depth), using experimental results of ref. 65. For lower crustal dike and sill intrusions, we used the primitive basalt composition from experimental results of ref. 66. We assumed an andesitic-dacitic composition for the upper crustal magma intrusions and used the non-linear relationship determined by ref. 29. To model the evolution of latent heat associated with phase change, we applied the predictor-corrector

algorithm and iterative approach[67] for the melt fraction-temperature relationships and employed under-relaxation to ensure numerical stability.

In order to focus on the entire crustal section, we neglect smaller-scale processes such as melt/gas extraction and thermo-mechanical feedbacks between the crust and the magma body during recharge[46,68]. We assume that the heat transfer is conductive and neglect the effects of shallow level hydrothermal circulation and internal magma chamber convection. In the upper crust, convecting hydrothermal fluids could potentially increase the rate of cooling and hence would require higher magma inputs to maintain magma bodies alive for the same duration. However, this effect will not be significant. The amount of heat that can be transferred from the magma reservoir to the surrounding host rock will be dominantly controlled by a conductive thermal boundary layer, containing insulating, warm wall rock, hence limiting the effect of internal convection and hydrothermal cooling[69] (Biot number $<<1$). Moreover, even assuming that convective hydrothermal cooling is efficient, it would not change the main conclusions of our work; the absolute numbers for fluxes that we find may be underestimated, but the influence of the lower crustal heating on the thermal maturation, and our comparison with other models (which also do not consider hydrothermal cooling) would stand.

We consider the long-term average magma flux and use average estimates for the geotherm, heat flux, and crustal thickness, although we acknowledge that these fluxes can vary over the lifetime of a magmatic province[70]. The characteristic thermal maturation timescales for a range of magma fluxes in stage I are given in Fig. 2b. In the present model, we use results of a fixed lower crustal magma flux from stage I and test a wide range of upper crustal magma fluxes at stage II. Using the results of a lower flux from stage I would result in a slight increase in the upper crustal flux estimates at stage II, but the order of magnitudes would be the same. We note

that the timescales and magma fluxes suggested in this study are conservative values in their conditions, and quantifying the effects of upper and lower crustal tectonic forces[31,52], additional enthalpy transferred from the lower crust in long timescales (>4 Myr), and temperature-dependent heat conductivity[29,71] can further increase the longevity of upper crustal magma reservoirs and decrease the estimates of upper crustal magma fluxes to keep them partially molten.

52 Karakas, O. & Dufek, J. Melt evolution and residence in extending crust: Thermal modeling of the crust and crustal magmas. *Earth and Planetary Science Letters* **425**, 131-144 (2015).

53 Patankar, S. *Numerical heat transfer and fluid flow*. (CRC Press, 1980).

54 Pollack, H. N., Hurter, S. J. & Johnson, J. R. Heat flow from the Earth's interior: analysis of the global data set. *Reviews of Geophysics* **31**, 267-280 (1993).

55 Pollack, H. N. & Chapman, D. S. On the regional variation of heat flow, geotherms, and lithospheric thickness. *Tectonophysics* **38**, 279-296 (1977).

56 Davies, J. H. Global map of solid Earth surface heat flow. *Geochemistry, Geophysics, Geosystems* **14**, 4608-4622 (2013).

57 Price, R. C. *et al.* Crustal and mantle influences and U-Th-Ra disequilibrium in andesitic lavas of Ngauruhoe volcano, New Zealand. *Chemical Geology* **277**, 355-373, doi:10.1016/j.chemgeo.2010.08.021 (2010).

58 Bailey, J. C., Jensen, E. S., Hansen, A., Kann, A. D. J. & Kann, K. Formation of heterogeneous magmatic series beneath North Santorini, South Aegean island arc. *Lithos* **110**, 20-36, doi:10.1016/j.lithos.2008.12.002 (2009).

59 Brady, R. J., Ducea, M. N., Kidder, S. B. & Saleeby, J. B. The distribution of radiogenic heat production as a function of depth in the Sierra Nevada Batholith, California. *Lithos* **86**, 229-244, doi:10.1016/j.lithos.2005.06.003 (2006).

60 Kumar, P. S. & Reddy, G. K. Radioelements and heat production of an exposed Archaean crustal cross-section, Dharwar craton, South India. *Earth and Planetary Science Letters* **224**, 309-324, doi:10.1016/j.epsl.2004.05.032 (2004).

61 Christensen, N. I. & Mooney, W. D. Seismic velocity structure and composition of the continental crust: a global view. *J. Geophys. Res.* **100**, 9761-9788 (1995).

62 L'ecuyer, P. Efficient and portable combined random number generators. *Communications of the ACM* **31**, 742-751 (1988).

63 Williams, M., Hanmer, S., Kopf, C. & Darrach, M. Syntectonic generation and segregation of tonalitic melts from amphibolite dikes in the lower crust, Striding-Athabasca mylonite zone, northern Saskatchewan. *Journal of Geophysical Research: Solid Earth (1978–2012)* **100**, 15717-15734 (1995).

64 Sisson, T., Ratajeski, K., Hankins, W. & Glazner, A. Voluminous granitic magmas from common basaltic sources. *Contributions to Mineralogy and Petrology* **148**, 635-661 (2005).

65 Piwinskii, A. & Wyllie, P. Experimental studies of igneous rock series: a zoned pluton in the Wallowa batholith, Oregon. *The Journal of Geology*, 205-234 (1968).

66 Nandedkar, R. H., Ulmer, P. & Müntener, O. Fractional crystallization of primitive, hydrous arc magmas: an experimental study at 0.7 GPa. *Contributions to Mineralogy and Petrology* **167**, 1-27 (2014).

67 Voller, V. & Swaminathan, C. General source-based method for solidification phase change. *Numerical Heat Transfer, 19B* 175-189 (1991).

68 Degruyter, W. & Huber, C. A model for eruption frequency of upper crustal silicic magma chambers. *Earth and Planetary Science Letters* **403**, 117-130, doi:http://dx.doi.org/10.1016/j.epsl.2014.06.047 (2014).

69 Carrigan, C. R. Biot number and thermos bottle effect: Implications for magma-chamber convection. *Geology* **16**, 771-774 (1988).

70 Paterson, S. R. & Ducea, M. N. Arc magmatic tempos: gathering the evidence. *Elements* **11**, 91-98 (2015)

71 Whittington, A. G., Hofmeister, A. M. & Nabelek, P. I. Temperature-dependent thermal diffusivity of the Earth's crust and implications for magmatism. *Nature* **458**, 319-321 (2009).

Figure 1 |

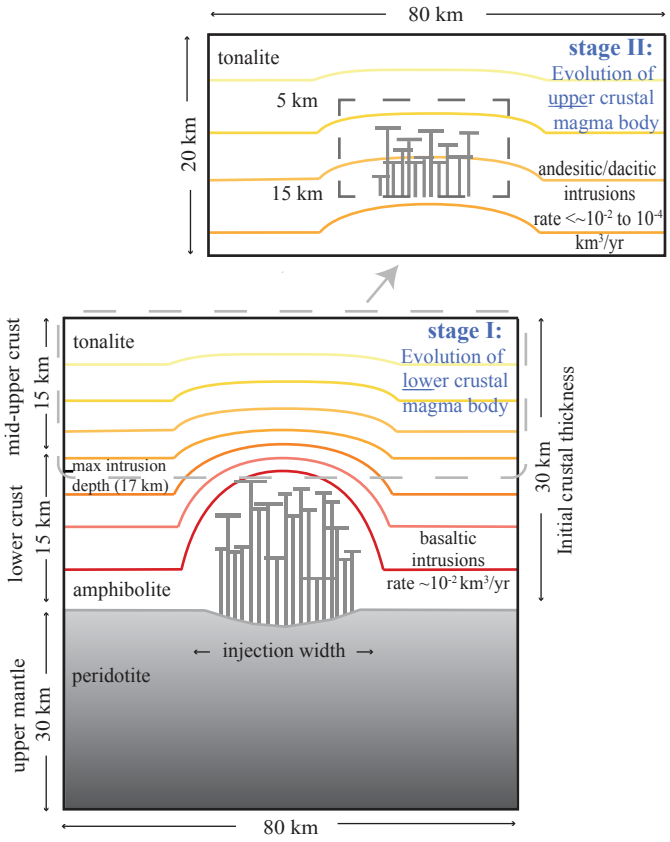
80 km
tonalite
stage II:
Evolution of
upper crustal
magma body
5 km
20 km
15 km
andesitic/dacitic
intrusions
rate <~10-2 to 10-4
km3/yr
tonalite
stage I:
Evolution of
lower crustal
magma body
mid-upper crust
15 km
max intrusion
depth (17 km)
lower crust
15 km
30 km
Initial crustal thickness
basaltic
intrusions
rate ~10-2 km3/yr
amphibolite
injection width
peridotite
upper mantle
30 km
80 km

Figure 2 |

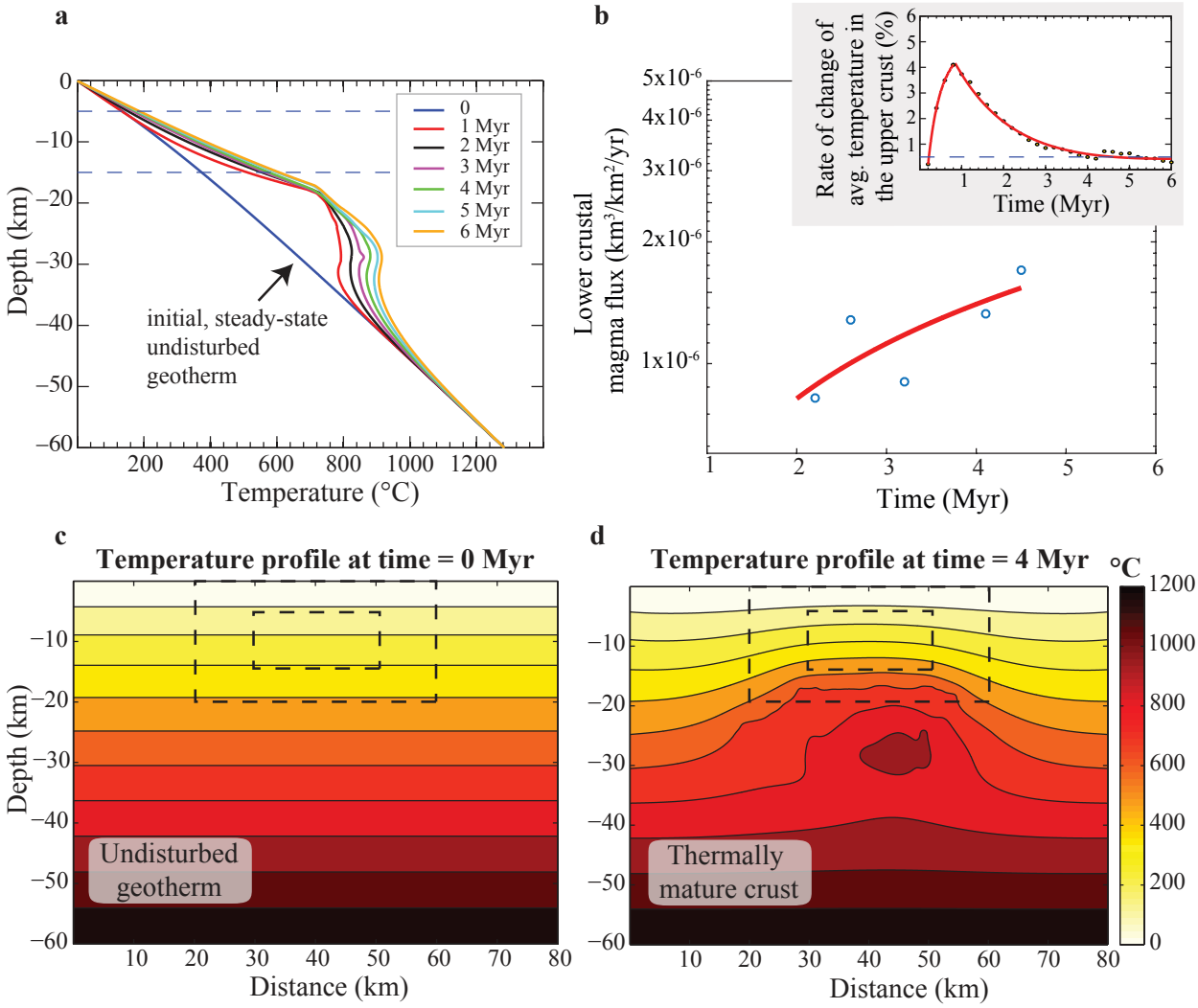
a
Depth (km)
Temperature (°C)
0
1 Myr
2 Myr
3 Myr
4 Myr
5 Myr
6 Myr
initial, steady-state
undisturbed
geotherm
b
Lower crustal
magma flux (km³/km²/yr)
Time (Myr)
Rate of change of
avg. temperature in
the upper crust (%)
Time (Myr)
c
Temperature profile at time = 0 Myr
Depth (km)
Undisturbed
geotherm
Distance (km)
d
Temperature profile at time = 4 Myr
°C
Thermally
mature crust
Distance (km)

Figure 3 |

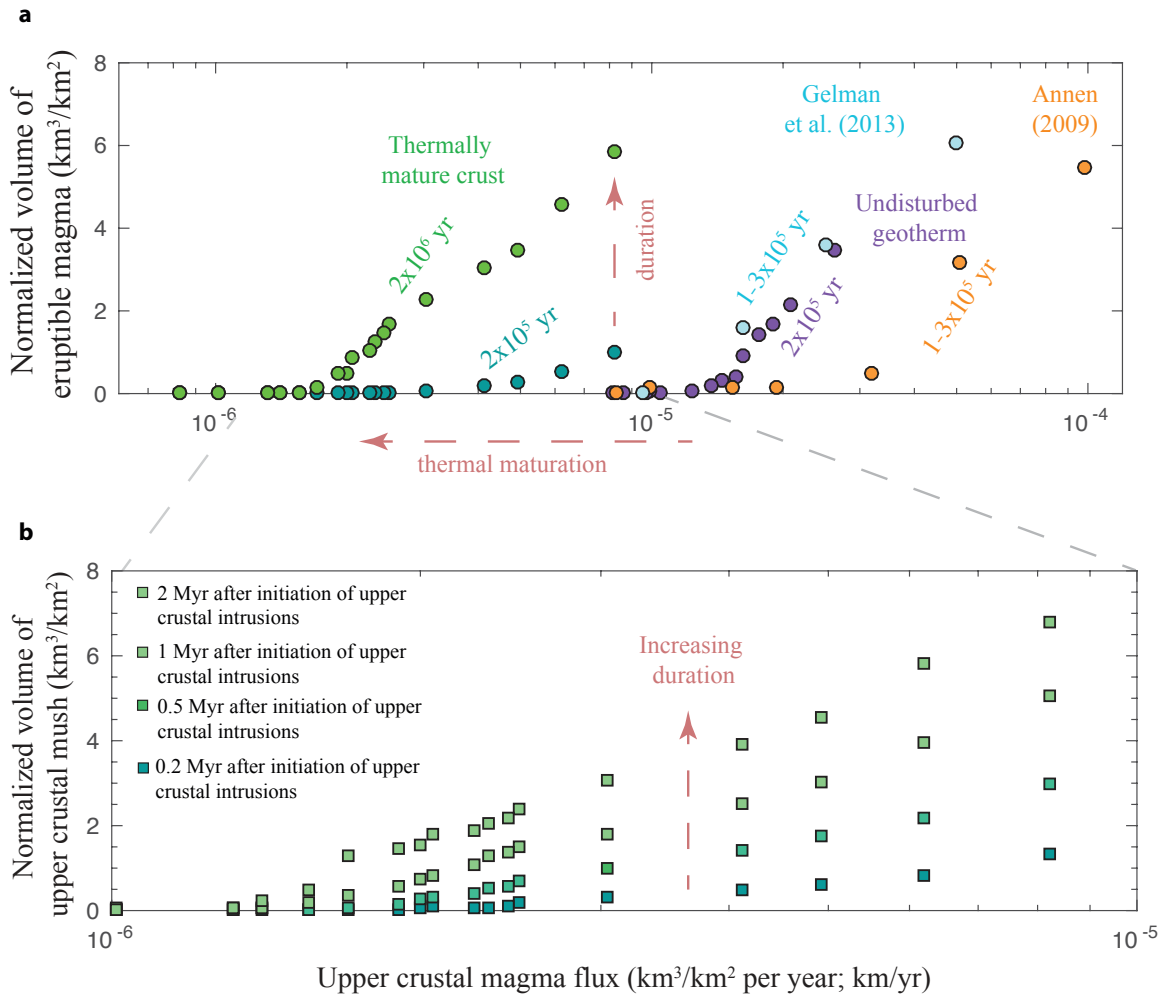
a
Normalized volume of eruptible magma (km³/km²)
Thermally mature crust
2x10⁶ yr
2x10⁵ yr
duration
Gelman et al. (2013)
Annen (2009)
Undisturbed geotherm
1-3x10⁵ yr
2x10⁵ yr
1-3x10⁵ yr
thermal maturation
b
Normalized volume of upper crustal mush (km³/km²)
2 Myr after initiation of upper crustal intrusions
1 Myr after initiation of upper crustal intrusions
0.5 Myr after initiation of upper crustal intrusions
0.2 Myr after initiation of upper crustal intrusions
Increasing duration
Upper crustal magma flux (km³/km² per year; km/yr)

Figure 4 |

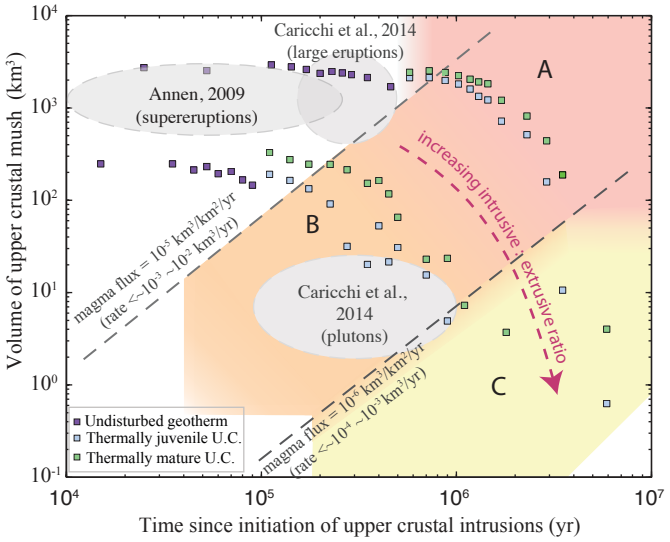
Caricchi et al., 2014
(large eruptions)
Annen, 2009
(supereruptions)
A
B
C
increasing intrusive / extrusive ratio
Caricchi et al.,
2014
(plutons)
magma flux = 10⁵ km³/km²/yr
(rate <~10⁻³ ~10⁻² km³/yr)
magma flux = 10⁵ km³/km²/yr
(rate <~10⁻⁴ ~10⁻³ km³/yr)
Undisturbed geotherm
Thermally juvenile U.C.
Thermally mature U.C.
Volume of upper crustal mush (km³)
Time since initiation of upper crustal intrusions (yr)

Extended Data Figure 1 |

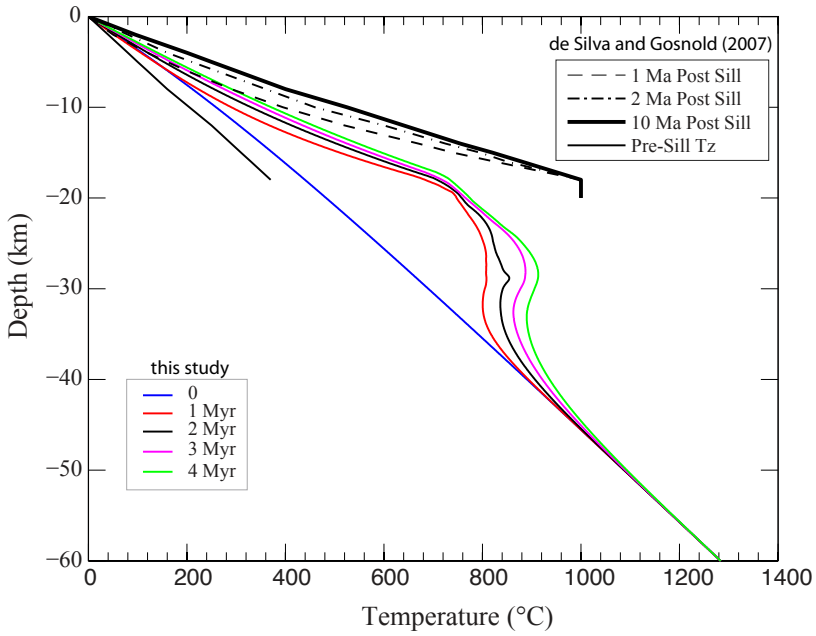

Extended Data Figure 2 |